



Contribution to the Themed Section: 'Revisiting Sverdrup's Critical Depth Hypothesis' Original Article

Sverdrup critical depth and the role of water clarity in Norwegian Coastal Water

D. L. Aksnes*

Department of Biology, University of Bergen and Hjort Centre for Marine Ecosystem Dynamics, Bergen N-5020, Norway

*Corresponding author: tel: +47 5558 4478; fax: +47 5558 4450; e-mail: dag.aksnes@bio.uib.no

Aksnes, D. L. Sverdrup critical depth and the role of water clarity in Norwegian Coastal Water. – ICES Journal of Marine Science, 72: 2041–2050.

Received 30 July 2014; revised 30 January 2015; accepted 4 February 2015; advance access publication 25 February 2015.

The critical depth concept was first recognized by Gran and Braarud (1935). During summer, in the Bay of Fundy, they observed an unexpected no bloom situation. Their interpretation was that high amounts of detritus of terrestrial origin caused too murky water and insufficient light for the tidally mixed phytoplankton. Almost 20 years later, this was elaborated by Sverdrup (1953) into a hypothesis for the initiation of the spring bloom in the North Atlantic Water (NAW) masses. Since then, variations in mixed layer depth have been a key in phytoplankton modelling. As illustrated by the study of Gran and Braarud, variation in the non-phytoplankton light attenuation coefficient is also a key to understand phytoplankton bloom conditions. Due to lack of accurate parameterizations, however, non-phytoplankton light attenuation is often assumed invariant in phytoplankton modelling. Here, I report spatial variation in a proxy for the pre-bloom light attenuation in Norwegian Coastal Water (NCW). It is shown that this variation can be partially accounted for by variations in salinity and dissolved oxygen. The light attenuation coefficient at 440 nm increased by 0.041 and 0.032 m^{-1} with drops in salinity and dissolved oxygen of 1PSU and 1 $\text{ml O}_2 \text{ l}^{-1}$, respectively. Consequences for the euphotic depth, Sverdrup critical depth, and the nutricline depth are discussed. I conclude that phytoplankton modelling, particularly across coastal and oceanic waters, such as NCW and NAW, needs to account for variations in the non-phytoplankton light attenuation and that salinity might be a useful proxy for regional parameterizations.

Keywords: light attenuation, oxygen, phytoplankton modelling, proxy, salinity, water column.

Introduction

Sverdrup's "critical depth" is commonly associated with the initiation of the spring bloom in clear oceanic water. This concept originated, however, from observations made in a murky inshore location, the Bay of Fundy (Gran and Braarud, 1935). There, elevated non-phytoplankton light attenuation, in combination with strong tidal mixing, was likely responsible for a no bloom situation at a time when both nutrients and incoming irradiance were at high levels (Figure 1). Based on a detailed study of phytoplankton and hydrography in the Gulf of Maine and the Bay of Fundy, Gran and Braarud (1935) concluded: "Although our material is insufficient for accurate calculations, we have come to the conclusion that for these reasons the extraordinary turbulence and turbidity conditions of the Bay of Fundy waters are the main factors for

limiting their production of phytoplankton. No other explanation could be found, as the surface waters at the least productive seasons, as in June, contain a surplus of nutrient salts, and the zooplankton feeding upon the phytoplankton is not as rich in the Bay of Fundy as in the gulf of Maine". This reasoning was translated (Sverdrup, 1953) into a mathematical expression for the critical depth (Z_{cr}) that has become a cornerstone, although questioned by some (e.g. Behrenfeld, 2010), in biological oceanography:

$$\frac{Z_{cr}}{1 - e^{-KZ_{cr}}} = \frac{1}{K} \frac{E_0}{E_c}, \quad (1)$$

where, in modern notation, K is the attenuation coefficient for downwelling irradiance, E_0 and E_c the average daily (24 h) irradiances, respectively, below the surface and at the compensation

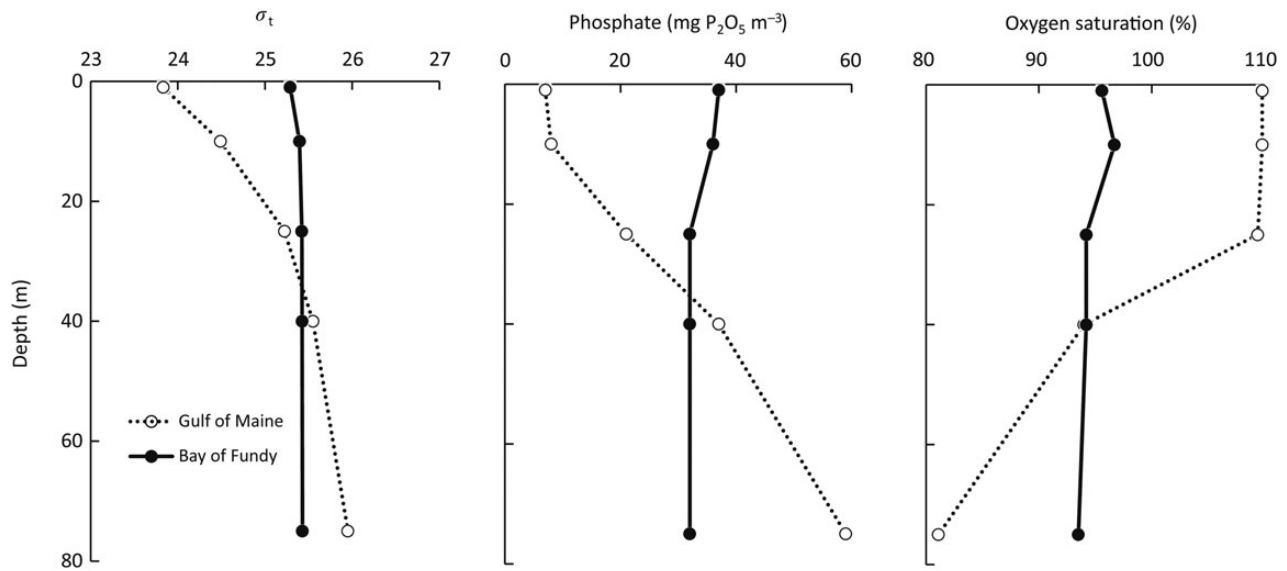


Figure 1. Birth of the critical depth concept. This concept originates from observations in the Bay of Fundy (Gran and Braarud, 1935), a location with high non-phytoplankton light attenuation and consequently a critical depth that might have been shallower than 50 m (see text). Compared with the Gulf of Maine, the Bay of Fundy was characterized by less stability (as indicated by σ_t), high nutrients and low oxygen saturation (i.e. low photosynthesis) throughout the water column. Gran and Braarud (1935) concluded that the phytoplankton in Bay of Fundy was limited by tidal mixing below a shallow compensation depth caused by limited light penetration. The observations for Gulf of Maine and Bay of Fundy are from June at station 24A and 37, respectively, and are taken from the tables in Gran and Braarud (1935).

depth, i.e. the depth where photosynthetic production equals “all” losses, not just respiration, during a 24-h cycle (see clarification by Chiswell, 2011). From Equation (1), we see that all coefficients in the critical depth formulation are associated with light and that the critical depth is particularly sensitive to variations in K . The frequently used phytoplankton bloom condition of Sverdrup (1953) can be formulated: if there exists a thoroughly mixed top layer of thickness D , D must be shallower than Z_{cr} in order for a bloom to develop.

Gran and Braarud (1935) noted that the high turbidity of the Bay of Fundy was due to detritus washed out by rivers at the head of the bay. They refer to an experiment on photosynthesis and respiration indicating that the compensation depth (Z_c) was not deeper than 10 m. If this depth, often equated with the euphotic depth, equals 1% light depth (i.e. $Z_c = -\ln(0.01)/K$), it can be seen that K must have been higher than 0.46 m^{-1} . This value indicates a critical depth shallower than 50 m, and it seems plausible that the lack of bloom in the Bay of Fundy indeed was in accordance with the critical depth hypothesis, i.e. that the mixed layer depth was deeper than the critical depth. Nevertheless, the observations of Gran and Braarud (1935) emphasize that natural variations in the non-phytoplankton light attenuation are critically important to phytoplankton bloom conditions. Sverdrup (1953) chose an oceanic test location, at Weather Ship M in the Norwegian Sea, with much higher water clarity than the Bay of Fundy. One challenge with this location, however, was the lack of observations of the pre-bloom light attenuation coefficient and Sverdrup had to assume values for this coefficient. Lack of accurate parameterizations of the non-phytoplankton light attenuation coefficient is still a challenge in ecosystem modeling in general as well as in coastal and oceanic areas off Norway (e.g. Schrum *et al.*, 2006; Hjøllø *et al.*, 2012; Samuelsen *et al.*, 2014).

Here, I quantify variations in the pre-bloom light attenuation in water masses along the coast of Norway (Table 1, Figure 2). These

water masses spanned salinities from 16.6 to 35.2. Norwegian Coastal Water (NCW) is transported with the Norwegian Coastal Current (NCC) from south to north (Figure 2) along the Norwegian coast (Sætre, 2007). NCW, characterized by salinity < 34.5 (Sætre, 2007), forms a wedge between the coastline and the North Atlantic Water (NAW, salinity > 34.5). Both NCW and NAW, which are located below the NCW, extend into the many deep fjords situated along the Norwegian coast on its way towards the Barents Sea. The freshwater content of the NCW originates from the brackish Baltic Sea, the rivers entering the North Sea, and drainage from Norway (Sætre, 2007). Many previous studies have shown that Chromophoric Dissolved Organic Matter (CDOM) of terrestrial origin is an important light absorber in the Baltic Sea, Kattegat, Skagerrak, and Danish coastal waters. This light absorption correlates negatively with salinity (e.g. Højerslev *et al.*, 1996; Stedmon *et al.*, 2000; Kowalczyk *et al.*, 2005), and as also reviewed by Nelson and Siegel (2013), CDOM absorption decreases linearly with increasing salinity if the mixing of offshore and terrestrial end-member water masses is the only process affecting CDOM. Based on this concept, I estimate an empirical model where salinity, but also dissolved oxygen (see below), serve as proxy for the non-phytoplankton NCW light attenuation.

Methods

During the unproductive winter season, locations along the Norwegian coast with bottom depth of several hundred meters (Table 1) contain relatively small amounts of organic and inorganic particles in the water column. Under these conditions, spectrophotometric measurements of light absorption in unfiltered samples have been used as proxy for the light attenuation of downwelling irradiance (Aksnes *et al.*, 2009). A benefit is that measurements can be obtained regardless of sunlight conditions and from large depths. All together, 375 measurements were obtained from 40 different locations along

Table 1. Sampling locations along the Norwegian coast in 2008.

Station number	Distance (km)	Location	Date	Latitude (North)	Longitude (East)	Bottom depth (m)
1102	0	Bunnefjorden	9 November	59°51.27	10°44.36	73
1100	25	Oslofjorden, Drøbak	8 November	59°38.38	10°37.50	194
1099	45	Breiangen	8 November	59°28.03	10°28.75	196
1097	101	Larvikfjorden	7 November	59°00.75	10°03.71	117
1095	128	Frierfjorden	7 November	59°06.36	9°37.05	89
1094	141	Eidangerfjorden, Brevik	7 November	59°01.33	9°44.81	107
1092	167	Off Kragerø	7 November	58°50.75	9°27.07	131
1091	184	Off Risør	6 November	58°44.26	9°15.34	183
1103	385	Gansfjorden	12 November	58°55.66	5°46.53	242
1105	414	Lysefjorden	13 November	59°00.20	6°16.54	454
1110	471	Sandsfjorden	13 November	59°30.64	6°15.41	422
1111	499	Nedstrandsfjorden	13 November	59°18.73	5°56.80	691
1112	527	Boknafjorden	13 November	59°09.99	5°33.11	574
1114	647	Hardangerfjorden, Tyssedal	15 November	60°07.29	6°32.87	150
1115	670	Hardangerfjorden, Ullensvang	15 November	60°19.51	6°38.00	353
1120	760	Fensfjorden	20 November	60°45.70	5°14.44	594
1123	773	Masfjorden	20 November	60°52.02	5°21.95	471
1127	813	Sognefjorden	21 November	61°08.52	5°49.92	1258
1128	900	Davikfjorden	24 November	61°54.63	5°34.78	576
1129	918	Hundvikfjorden	24 November	61°52.22	5°55.21	358
1130	946	Innvikfjorden	24 November	61°49.22	6°26.70	436
1133	1013	Vanylvsfjorden	25 November	62°08.09	5°20.99	254
1141	1030	Syvdsfjorden	26 November	62°10.99	5°39.24	375
1145	1071	Storfjorden 1	26 November	62°24.73	6°26.19	402
1146	1101	Storfjorden 2	26 November	62°26.74	6°50.06	669
1148	1143	Geirangerfjorden	26 November	62°05.48	7°03.88	185
1151	1209	Romsdalsfjorden	29 November	62°40.76	7°04.95	471
1154	1243	Langfjorden	30 November	62°43.55	7°45.27	353
1157	1273	Tingsvollfjorden	1 December	62°56.41	8°07.08	308
1160	1289	Freifjorden	1 December	63°01.03	7°50.80	135
1162	1304	Talgsjøen	2 December	63°08.90	7°52.16	327
1163	1413	Trondheimsfjorden	3 December	63°37.24	9°46.97	600
1166	1483	Beistadfjorden	4 December	63°55.12	11°02.57	239
1205	1642	Tosenfjorden	16 December	65°10.19	12°37.81	525
1202	1656	Bindalsfjorden	15 December	65°10.31	12°18.74	699
1196	1743	Vefsnfjorden	14 December	65°51.52	13°10.52	151
1191	1804	Ranafjorden	13 December	66°15.07	13°44.39	425
1185	1867	Glomfjorden	11 December	66°49.10	13°37.05	372
1175	1963	Follafjorden	8 December	67°33.03	14°46.42	487
1184	2055	Ofotfjorden	10 December	68°16.34	15°50.72	608

Distance is the approximate distances from station 1102.

the Norwegian coast (Table 1, Figure 2) between 58°N and 68°N during a cruise with RV “Håkon Mosby” in the period from 6 November to 16 December 2008. This period of the year was chosen to minimize the effect from phytoplankton on light attenuation. Depending on the bottom depth (Table 1), 6–12 water samples were collected between the surface and 700-m depth with rosette mounted Niskin water collectors attached to a CTD system (Seabird SBE 911). Absorbance on the unfiltered water samples (A_{un}) was measured at 400, 420, 440, 450, 460, 480, 500, and 550 nm with a spectrophotometer (UV/VIS Spectrometer Lambda 2, Perkin Elmer). Absorbance readings were made for four subsamples placed in a 10-cm quartz cuvette that was acclimatized to room temperature. Distilled freshwater purified with a Millipore Simplicity 185 Water Purification System was used as blank control. As in studies of light absorption (e.g. Højerslev *et al.*, 1996), I calculated a quantity (in units of m^{-1}) from the absorbance readings; $a_{\text{un}}(\lambda) = 2.303A_{\text{un}}(\lambda)/0.1$, where λ is the wavelength. I fitted the exponential function, $a_{\text{un}}(\lambda) = Ce^{-k\lambda}$, to the observations by log-linear regression (Bricaud *et al.*, 1981). Here, C is a constant

and k is the spectral slope factor. Throughout the present study, I use a_{un} at 440 nm, which was obtained by insertion of $\lambda = 440$ in the estimated regression equations. This wavelength was chosen because it is approximately the midpoint of the waveband peak that most classes of algae have in their photosynthetic action spectrum (Kirk, 2011). Similar to the attenuation of downwelling irradiance, K , the a_{un} measurements are affected by scattering and absorption from potential particles, such as phytoplankton, as well as from dissolved matter of the water samples. Thus, below I avoid to use the notation of absorption (a) and instead use K_p to emphasize that the measurements are used as an “approximation” for the attenuation coefficient (K) for downwelling irradiance (at 440 nm), i.e. $K \approx K_p = a_{\text{un}}(440)$. This approximation ignores that K is an apparent optical property that depends on the angular distribution of the underwater light field. The ability of the proxy, K_p , to predict measured light penetration is tested for a NAW and a NCW location (see below).

Dissolved oxygen was determined from the water samples by a standard Winkler technique, and salinity was obtained from the CTD system simultaneously with the collection of water. Water

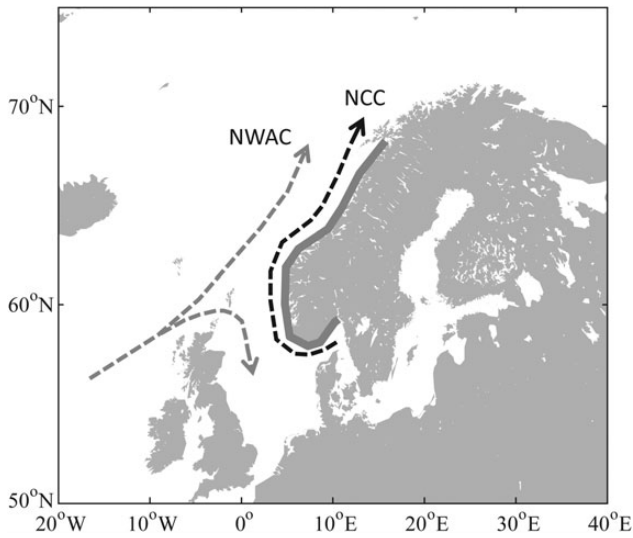


Figure 2. The Norwegian Atlantic Current (NWAC) transports saline NAW into the Norwegian Sea, whereas the NCC transports less-saline NCW northwards along the Norwegian coast. The shaded area indicates the area covered by the stations listed in Table 1.

samples (100 ml) were also filtered through 0.45 μm Sartorius filters, and the filters were frozen for later determination of Chl *a* by the use of acetone extraction (Holm-Hansen *et al.*, 1965).

Model used in estimation

The chlorophyll concentrations were generally low (see below), but chlorophyll (Chl) will nevertheless affect the proxy for light attenuation K_p . I apply the following model:

$$K_p = K_{\text{non}} + f(\text{Chl}), \quad (2)$$

where K_{non} is the non-phytoplankton light attenuation and $f(\text{Chl})$ the attenuation from algal cells (see Table 2 for a summary of symbols).

I assume that the water samples of NCW are a mixture of two end-member water masses; oceanic water (NAW) and freshwater (FW). Furthermore, it is assumed that K_{non} is determined by the mixing ratio of the two water masses and the respective non-phytoplankton attenuations, K_{NAW} and K_{FW} , according to:

$$K_{\text{non}} = gK_{\text{NAW}} + (1 - g)K_{\text{FW}} + K_{\text{loc}}, \quad (3)$$

where g and $1 - g$ are the fractions of NAW and FW, respectively (as given by salinity, see below). This model is similar to conservative mixing of, e.g. CDOM of two end-member water masses, which gives rise to a negative linear relationship between CDOM absorption and salinity (Aarup *et al.*, 1996; Kowalczyk *et al.*, 2003; Stedmon and Markager, 2003; Nelson and Siegel, 2013). Equation (3) is a simplification since the freshwater sources and their content of persistent light attenuating substances are diverse and include many different riverine inputs to the Baltic Sea, the North Sea, as well as directly to the NCW. The third term of Equation (3), K_{loc} , is introduced to reflect locally produced non-phytoplankton light attenuating substances from heterotrophic activity. Previous oceanic (Yamashita and Tanoue, 2008; Nelson and Siegel, 2013) and fjord (Aksnes *et al.*, 2009) studies suggest that heterotrophic consumption of dissolved oxygen, i.e. apparent oxygen utilization (AOU, Nelson and Siegel, 2013), might serve as proxy for light absorption in some

Table 2. Symbols used in the text.

A_{un}		Observed light absorbance of unfiltered water samples
a_{un}	m^{-1}	Light absorption of unfiltered water samples
Chl	mg m^{-3}	Concentration of chlorophyll <i>a</i>
FW		Freshwater draining to NCW
g		Fraction of NAW in NCW (=Sal/35.2)
h		= Oxy/7.1
Λ	nm	Wavelength
K	m^{-1}	Attenuation coefficient for downwelling irradiance
K_p	m^{-1}	Proxy for K [$K_p = a_{\text{un}}(440)$]
K_{non}	m^{-1}	Non-chlorophyll light attenuation coefficient
K_{FW}	m^{-1}	Non-chlorophyll light attenuation of the FW source
K_{NAW}	m^{-1}	Non-chlorophyll light attenuation of the NAW source
K_{loc}	m^{-1}	Non-chlorophyll light attenuation of local substances
$K_{\text{Oxy}=0}$	m^{-1}	Non-chlorophyll light attenuation associated with no dissolved oxygen
NAW		North Atlantic Water
NCC		Norwegian Coastal Current
NCW		Norwegian Coastal Water
Oxy	ml l^{-1}	Dissolved oxygen concentration
Oxy_{max}	ml l^{-1}	The maximal dissolved oxygen in the dataset (7.1 ml l^{-1})
Sal		Salinity

areas. The present study includes hypoxic fjord basins and it is hypothesized that bacterial degradation of particulate organic matter produces local light attenuating DOM in proportion with the removal of dissolved oxygen. Such relationship between light attenuation and AOU is parameterized as follows: for a water mass high in dissolved oxygen ($\text{Oxy} = \text{Oxy}_{\text{max}}$), $K_{\text{loc}} = 0$ is assumed. When $\text{Oxy} < \text{Oxy}_{\text{max}}$, K_{loc} is assumed to increase linearly with the decrease in Oxy, i.e. $K_{\text{loc}} = (1 - h)K_{\text{Oxy}=0}$, where $h = \text{Oxy}/\text{Oxy}_{\text{max}}$ and $K_{\text{Oxy}=0}$ is the hypothetical non-phytoplankton light attenuation of water without dissolved oxygen. Equation (3) then becomes:

$$K_{\text{non}} = gK_{\text{NAW}} + (1 - g)K_{\text{FW}} + (1 - h)K_{\text{Oxy}=0}. \quad (4)$$

Estimation of model parameters

The salinity of the NAW end-member is set equal to the highest salinity (35.2) observed in the present study and the salinity of FW end-member is set to zero. Then, $g = \text{Sal}/35.2$, where Sal is the salinity of the water sample in question. Similarly, Oxy_{max} is set equal to the highest dissolved oxygen concentration in the dataset (7.1 ml l^{-1}) and consequently $h = \text{Oxy}/7.1$.

The water samples were collected during a period of presumably low biological productivity (November and December), but Chl *a* was present (average 0.23 and s.d. 0.49 mg m^{-3}) particularly in the southernmost locations (see the ‘‘Results’’ section). Out of the 375 samples, 324 contained concentrations less than 0.5 mg m^{-3} and 26 samples had concentrations on the range 1–3.6 mg m^{-3} . The effect of chlorophyll on K is known to be non-linear (Morel and Maritorena, 2001). To keep the number of parameters to be estimated low, however, I assume that the effect of chlorophyll (Chl) on K_p is linear and Equation (2) becomes $K_p = K_{\text{non}} + k_3\text{Chl}$. Combination with Equation (4) and elimination of

g and h by insertion of $g = \text{Sal}/35.2$ and $h = \text{Oxy}/7.1$ provide the following model:

$$K_p = k_0 + k_1 \text{Sal} + k_2 \text{Oxy} + k_3 \text{Chl}, \quad (5a)$$

where k_0 , k_1 , and k_2 are:

$$k_0 = K_{\text{FW}} + K_{\text{Oxy}=0}, \quad (5b)$$

$$k_1 = \frac{K_{\text{NAW}} - K_{\text{FW}}}{35.2}, \quad (5c)$$

$$k_2 = \frac{-K_{\text{Oxy}=0}}{7.1}. \quad (5d)$$

Estimates of k_0 , k_1 , k_2 , and k_3 were obtained by fitting Equation (5a) to the observations of K_p , Sal, Oxy, and Chl. This equation corresponds to a linear multiple regression model and the software Statistica was applied. Estimates of K_{NAW} , K_{FW} , and $K_{\text{Oxy}=0}$ were obtained by solving Equations (5b)–(5d).

Observed and predicted light penetration in pre-bloom NAW and NCW

Measurements of underwater irradiance (Trios RAMSES ACC hyperspectral radiometer), salinity, dissolved oxygen, and fluorescence in NCW and NAW were available from two field studies. In the first, measurements were taken at a coastal location (60.41°N 5.10°E, 9 February 2010) during a cruise with RV “H. Mosby”. The second included measurements from a cruise with RV “G.O. Sars” at a station in the Norwegian Sea (65.03°N 0.51°W, 7 May 2013). The observed light penetration was compared with that predicted from the proxy, K_p . Values for K_p as a function of depth were obtained from Equation (5a) by use of observed depth distributions of salinity, dissolved oxygen, and chlorophyll as input. The predicted irradiance, E , as a function of depth (z) was calculated:

$$E = E_0 \exp\left(-\int_0^z K_p(\sigma) d\sigma\right). \quad (6)$$

Here, E_0 is the irradiance just below the surface and σ is an integration variable accounting for the observed non-uniform depth distributions of K_p (being a function of salinity, dissolved oxygen, and chlorophyll).

Results

The variations in salinity, oxygen, and chlorophyll accounted for 62% ($R = 0.79$) of the observed variation in the light attenuation proxy, K_p , and the statistical effects of all three variables were significant (Figure 3 and Table 3). Increases of 0.041 ± 0.003 and $0.032 \pm 0.004 \text{ m}^{-1}$ in K_p are associated with a 1 PSU drop in salinity and a 1 ml l^{-1} drop in dissolved oxygen, respectively (Table 3). The estimated effect of chlorophyll corresponds to an increase of $0.073 \pm 0.011 \text{ m}^{-1}$ for an increase of $1 \text{ mg Chl } a \text{ m}^{-3}$ (Table 3). The estimated non-phytoplankton light attenuation of the freshwater source was $K_{\text{FW}} = 1.47 \pm 0.05 \text{ m}^{-1}$. The corresponding value for the North Atlantic source water was $K_{\text{NAW}} = 0.03 \pm 0.07 \text{ m}^{-1}$.

Overall, the observed K_p tends to decrease with latitude and depth (Figure 4), and this pattern is also well reflected by the model predicted K_p (Figure 5a). Figure 5b–d illustrates how the predicted K_p is associated with variations in chlorophyll, salinity, and dissolved oxygen, respectively. Except for the surface water of the southernmost locations, chlorophyll concentrations were generally

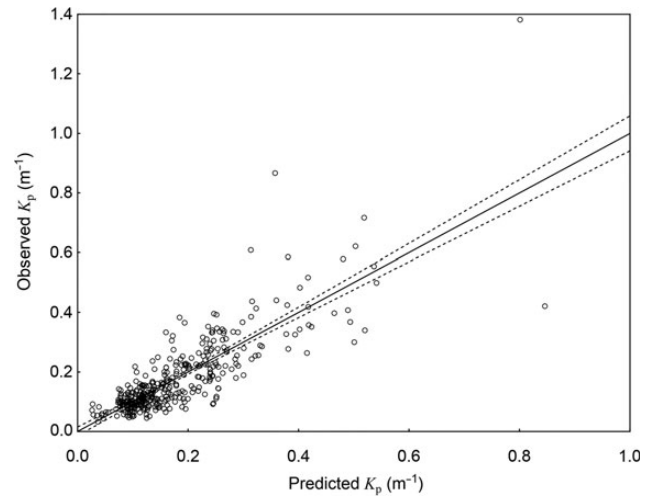


Figure 3. Model predicted vs. observed K_p at 440 nm. The model predictions are: $K_p = 1.70 + 0.073 \text{ Chl} - 0.041 \text{ Sal} - 0.032 \text{ Oxy}$, $r = 0.79$, $p < 10^{-5}$, $n = 375$ (Table 3). Dotted lines represent 95% CI.

Table 3. Statistical effects of salinity, oxygen, and chlorophyll on K_p (440 nm) estimated with multiple regression analysis according to the model in Equation (5).

Coefficient and unit	Estimates	β
$k_0 \text{ m}^{-1}$	1.70 ± 0.09	
$k_1 \text{ m}^{-1}(\text{PSU})^{-1}$	-0.041 ± 0.003	-0.62 ± 0.04
$k_2 \text{ m}^{-1}(\text{ml O}_2 \text{ l}^{-1})^{-1}$	-0.032 ± 0.004	-0.27 ± 0.03
$k_3 \text{ m}^{-1}(\text{mg Chl } a \text{ m}^{-3})^{-1}$	0.073 ± 0.011	0.27 ± 0.04
$K_{\text{Oxy}=0} \text{ m}^{-1}$	0.23 ± 0.03	
$K_{\text{FW}} \text{ m}^{-1}$	1.47 ± 0.05	
$K_{\text{NAW}} \text{ m}^{-1}$	0.03 ± 0.07	

All effects were statistically significant ($p < 10^{-5}$). The multiple R was 0.79. The β is the regression coefficient that is obtained when all variables are standardized to a mean of 0 and an s.d. of 1. This coefficient compares the relative contribution of each independent variable (salinity, dissolved oxygen, and Chl a) in the prediction of K_p . The indicated uncertainties are \pm standard error. The estimates are based on 375 records where the ranges of the variables were K_p 0.03–1.4 m^{-1} (mean 0.18), salinity 16.6–35.2 (mean 33.4), chlorophyll 0.0–3.6 $\text{mg Chl } a \text{ m}^{-3}$ (mean 0.23), and dissolved oxygen 0.1–7.1 ml l^{-1} (mean 5.21).

low and therefore accounted for a small part of the variations in K_p in the model (Figure 5b). The variations in salinity accounted for the largest variations in K_p (Figure 5c), except for some intermediate and large depths where variations in oxygen, particularly in the south, accounted for the largest part of the variations in K_p (Figure 5d).

The derived model was verified by measurements obtained at an NCW and an NAW location (Figure 6). Light penetrations, standardized as the fraction of observed irradiance at 2-m depth, are shown in Figure 6a. The sensitivity of the radiometer allowed irradiance measurements down to 80 m at the NCW location and to 170 m in the clearer NAW location. Linear regression analysis on the ln-transformed irradiances (not shown in Figure 6a) gave attenuation coefficients (K) of 0.182 m^{-1} (s.e. = 0.002, $r^2 = 0.99$, $n = 17$) and 0.0600 m^{-1} (s.e. = 0.0007, $r^2 = 0.99$, $n = 22$) for the NCW and the NAW location, respectively.

The light penetration [Equations (5) and (6)] predicted from the observed distributions of salinity (Figure 6b), dissolved oxygen

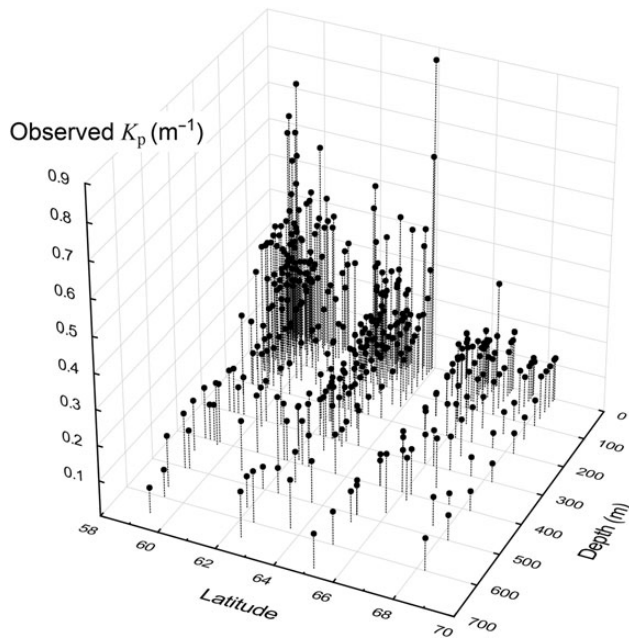


Figure 4. Observations of K_p at 440 nm as a function of latitude and depth. One observation, $K_p = 1.38 \text{ m}^{-1}$ (Figure 3), is outside the scale and not shown.

(Figure 6c), and fluorescence (Figure 6d) is shown by the lines in Figure 6a. The average of the predicted attenuation coefficients (i.e. K_p) are 0.185 and 0.064 m^{-1} for NCW (0–80 m) and NAW (0–170 m), respectively, which are close to the measured values.

The fluorescence measurements (Figure 6d) indicate chlorophyll concentrations below 0.05 and $0.22 \text{ mg Chl } a \text{ m}^{-3}$ at the NCW and the NAW location, respectively. An estimate of the non-phytoplankton attenuation, K_{non} , is obtained by setting $\text{Chl} = 0$ in Equation (5a):

$$K_{\text{non}} = 1.70 - 0.041\text{Sal} - 0.032\text{Oxy}. \quad (7)$$

This provides K_{non} values of 0.183 m^{-1} and 0.054 for the NCW and the NAW location, respectively.

The average salinity was 35.12 and 32.55 for NAW (upper 170 m) and NCW (upper 80 m), respectively (Figure 6b). According to the proxy model, $\sim 80\%$ of the elevated K_{non} at the NCW location was associated with the lower salinity, whereas the remaining 20% was associated with lower dissolved oxygen at this location (Figure 6c).

The effect of chlorophyll on K has been estimated by Morel and Maritorena (2001) and for 440 nm this effect corresponds to $K_{\text{Chl}} = 0.11 \text{ Chl}^{0.67}$. It should be noted that this expression also includes effects of constituents other than chlorophyll like CDOM produced by algal cells. Subtraction of this effect (insertion of average chlorophyll of the observed profiles in Figure 6d) from the measured K values provides K_{non} values of 0.168 and 0.032 m^{-1} for the NCW and NAW location, respectively, which is lower than those indicated by the proxy.

Discussion

The present study provides a model to estimate variations in the non-phytoplankton light attenuation in coastal waters of Norway in relation to the variations in salinity and dissolved oxygen.

Because the largest salinity variation is generally found in upper water, salinity appears to be a useful proxy for K_{non} in the euphotic zone. The largest variation in dissolved oxygen is normally found at intermediate and large depths, i.e. where hypoxia is common, and has been applied as proxy for the light conditions in the mesopelagic zone (Aksnes *et al.*, 2009). Salinity has previously been applied as proxy for non-phytoplankton light attenuation in phytoplankton modelling, e.g. in Florida shelf water (Walsh *et al.*, 2003) and in the Gulf of St Lawrence (Mei *et al.*, 2010). These studies report salinity coefficients, which corresponds to $k_1 = -0.041 \pm 0.003 \text{ m}^{-1} \text{ PSU}^{-1}$ (Table 3), on the ranges -0.095 to -0.003 (for 443 nm) and -0.02995 to $-0.01392 \text{ m}^{-1} \text{ PSU}^{-1}$ (for PAR). The present study suggests that salinity also might be a useful proxy for K_{non} in phytoplankton modelling in coastal waters of Norway. Below, I discuss some implications of variation in K_{non} on the euphotic depth, the critical depth, and the nutricline depth spanning a salinity range from 28 to 35 (Figure 7).

Implications of variation in the non-phytoplankton light attenuation of NCW

If the depth of the euphotic zone is defined as the depth where 1% of the surface light penetrates, the euphotic depth of NCW₂₈ (i.e. salinity is 28) is 98 m shallower than in NAW₃₅ (14 and 112 m, respectively, Figure 7) for a water column devoid of chlorophyll and with a dissolved oxygen concentration of 7 ml l^{-1} . According to the assumptions underlying Figure 7 (see legend), the deepening of the critical depth associated with a move from NCW₂₈ to NAW₃₅ is 427 m (from 61 to 488 m). Note, however, that the actual shoaling in a bloom situation will also be affected by the phytoplankton shading.

Elevated non-phytoplankton attenuation shoals the euphotic zone and consequently also the phytoplankton and nutrient distributions (Urtizberea *et al.*, 2013). This optical effect is strong and can be quantified by the analytical expression for the steady-state nutricline depth (Z_n); $Z_n = -\ln(\psi K)/K$ [Equation (3) in Aksnes *et al.*, 2007], where ψ is a scaled quantity reflecting biological nutrient uptake rate, vertical transport of the nutrient, and the actual definition of the nutrient concentration at Z_n . For $\psi = 0.014 \text{ m}$ (Figure 1 in Aksnes *et al.*, 2007), nutricline depths corresponds to 16 and 182 m for the K_{non} values calculated for NCW₂₈ and NAW₃₅, respectively (Figure 7). This calculation is based solely on the change in K_{non} and ignores the effect of phytoplankton self-shading. Nevertheless, it illustrates that spatial variations in K_{non} are likely to have large implications for the vertical distribution of nutrients in NCW during the productive season.

The simple analytical sensitivity analysis in Figure 7 illustrates that the largest variations (in meters) in euphotic depth, critical depth, and nutricline depth are to be expected at salinity variations in the upper range (i.e. between 34 and 35). This is in line with previous sensitivity analyses involving numerical ecosystem models (e.g. Fasham *et al.*, 1990; Urtizberea *et al.*, 2013) showing that the outcome of these models, particularly at small values of K_{non} (i.e. close to pure water), is very sensitive to variation in K_{non} . This can be illustrated by assumptions made by Sverdrup (1953). He assumed values in the range 0.075 – 0.10 m^{-1} for his critical depth estimates for the Norwegian Sea. A value of 0.05 m^{-1} , which appears realistic for the NAW pre-bloom situation (see above), provides critical depths that are 50–100% deeper than those indicated by Sverdrup and will, for a given mixed layer depth, indicate earlier spring bloom initiation than in Sverdrup (1953).

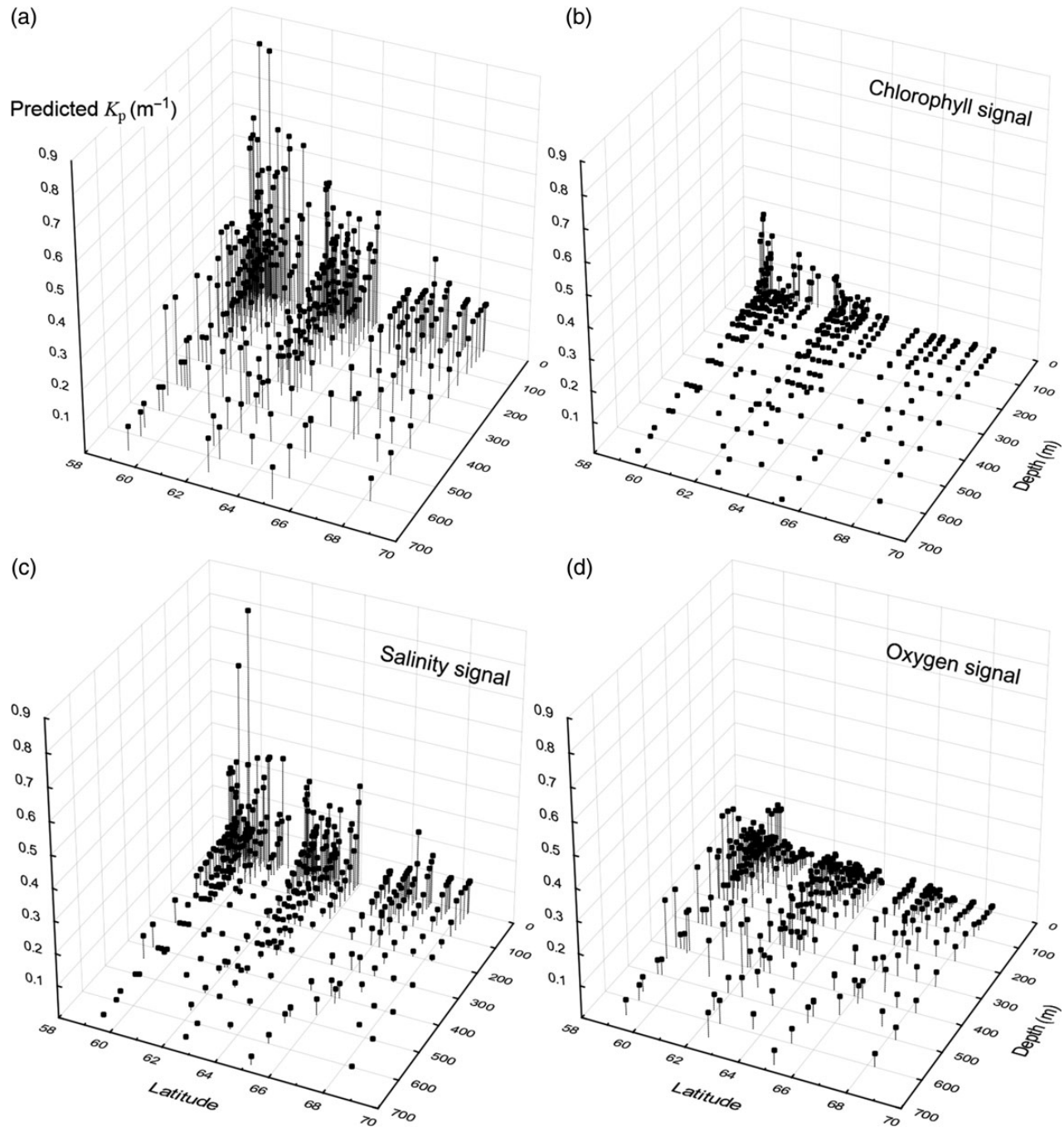


Figure 5. The model predicted K_p values at 440 nm [Equation (5a), estimated coefficients in Table 3] as a function of latitude and depth (a), and how much of these values that could be accounted for by chlorophyll (b), salinity (c), and dissolved oxygen (d).

Salinity as proxy for non-phytoplankton attenuation in ecological modelling

According to Sarmiento and Gruber (2006) and Fujii *et al.* (2007), most ecosystem models that have been developed to study the ocean's biogeochemical properties use simple formulations to describe light penetration. In such formulations (Sarmiento and Gruber, 2006), K is often a function of the simulated phytoplankton concentration added to the contribution from clear water (K_w) and non-phytoplankton constituents (K_x), i.e. $K = K_w + K_x + k_p P$, where $k_p P$ is the contribution from phytoplankton ($K_w + K_x$ here

corresponds to K_{non}). The effect of pure water is often set close to 0.04 m^{-1} for PAR, while, according to Sarmiento and Gruber (2006), K_x is generally ignored. Some ecological modelling studies do include the optical effects (and thereby K_x) of constituents such as CDOM (Bissett *et al.*, 1999; Fujii *et al.*, 2007; Mouw *et al.*, 2012; Alver *et al.*, 2014). A reason why the more advanced bio-optical approaches are underrepresented in ecosystem models is likely due to the difficulty and uncertainties in translating model outputs accurately into optical properties. Given that there exists a robust relationship between non-phytoplankton light

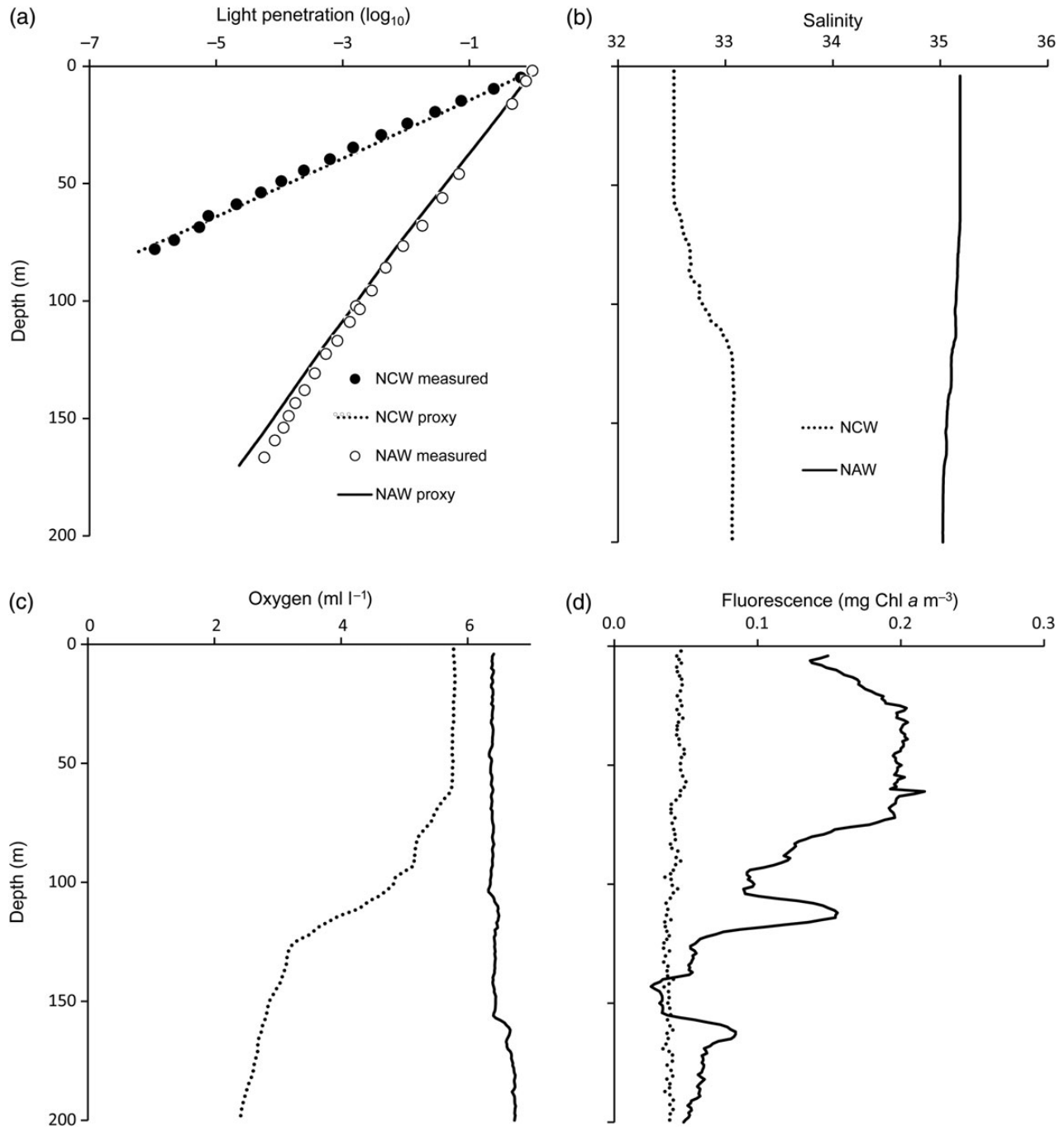


Figure 6. Observed and model predicted light penetration (a) in NAW (65.03°N 0.51°W on 7 May 2013) and in NCW (60.41°N 5.10°W on 9 February 2010). Light penetration is given as a fraction; $E(z)/E(2)$, where $E(z)$ and $E(2)$ are the observed downwelling irradiance at depth z and 2 m, respectively. The model predicted light penetration was obtained by using Equation (5a) (estimated coefficients in Table 3) and the observed distributions of salinity (b), dissolved oxygen (c), and chlorophyll (d).

attenuation and salinity for certain areas (e.g. Walsh *et al.*, 2003; Mei *et al.*, 2010), salinity proxies for non-phytoplankton attenuation are likely to be useful. This is particularly true if assumption of invariant K_{non} is the alternative. It should be noted, however, that there is no universal relationship between the non-phytoplankton light attenuation and salinity and that Equation (7) has been derived specifically for the pre-bloom situation in Norwegian coastal areas.

Latitudinal variations in non-phytoplankton light attenuation

A large fraction (38%) of the variation in the light attenuation proxy is not accounted for by the variations in salinity, oxygen, and chlorophyll (Table 3 and Figure 3). The measurements were obtained between the surface and 700-m depth along a coastline that spans 2000 km (Table 1). Variation in attenuation properties of the

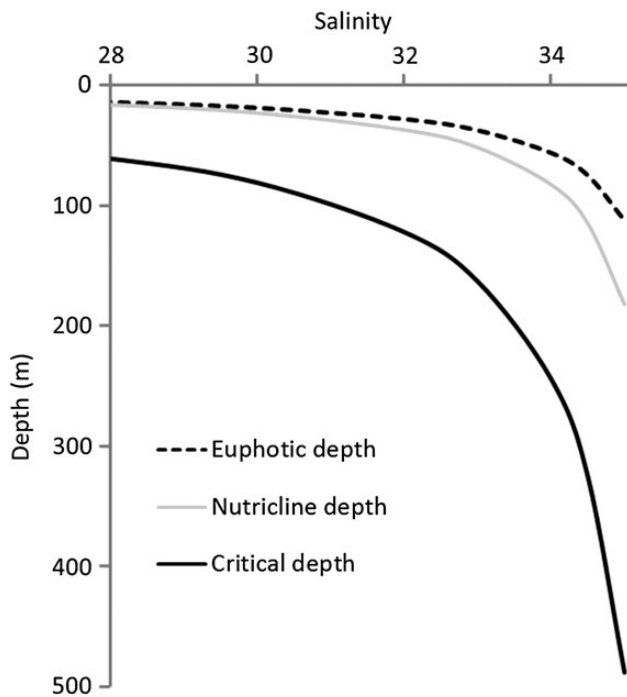


Figure 7. Predicted variations in euphotic, nutricline, and critical depth as a function of salinity in a gradient from NCW₂₈ to NAW₃₅. Euphotic depth was calculated according to $-\ln(0.01)/K$, nutricline depth according to $-\ln(0.014K)/K$ (see text), and critical depth according to Equation (1), where $E_0/E_c = 20$ (see text). K was derived from salinity according to the proxy equation (7) where dissolved oxygen was set constant ($Oxy = 7 \text{ ml l}^{-1}$).

different freshwater sources along this coastline is likely to have affected the observations, but also variations in the oceanic waters that mix in along the coast. Such effects have not been accounted for in the present analysis and have likely increased the error term of the estimation model. If the distance along the coast from south to north (Table 1) is included *ad hoc* in Equation (5a), this effect, as well as the other three, becomes statistically significant ($p < 10^{-5}$), and the unexplained fraction drops from 38 to 33%. The distance effect is negative, -0.058 m^{-1} per 1000 km. This might indicate that the non-phytoplankton light attenuation of the freshwater and/or the oceanic sources drops northward along the coast. This suggestion, however, needs to be addressed in studies where the optical properties of these sources are targeted.

Effects of terrestrial CDOM on non-phytoplankton light attenuation in NCW

CDOM has received increased attention in the last decades due to its role in the global carbon budget, but also because it changes the colour (brownification) and light conditions in rivers and streams (Roulet and Moore, 2006), in lakes (Larsen *et al.*, 2011), and in coastal waters (Branco and Kremer, 2005; Frigstad *et al.*, 2013). Increased amounts of organic carbon in Scandinavian lakes have been related to increased precipitation, warming, and associated changes in the terrestrial vegetation (Larsen *et al.*, 2011). Long-term Secchi depth shoaling off Southern Norway, in the North Sea, and in the Baltic Sea has been reported (Fleming-Lehtinen and Laamanen, 2012; Dupont and Aksnes, 2013) and associated with long-term ecosystem changes (Haraldsson *et al.*, 2012), but it is unclear to what extent this shoaling has been caused by increased phytoplankton or CDOM of

terrestrial origin. Predictions based on climate change scenarios suggest future increase in organic carbon in lakes and rivers in Scandinavia (Larsen *et al.* 2011) and consequently to an increase in the coefficient K_{FW} of the mixing model. In that case, K_{non} increases and is likely to cause shoaling and narrowing of NCW photic zones in the coming years. In the words of Gran and Braarud (1935): “The amount was so considerable that it seemed obvious that the detritus essentially must lower the light supply of subsurface localities”.

Acknowledgements

Thanks to Mette Hordnes for cruise participation, sampling, and laboratory analyses, to Rita Amundsen (University of Oslo) for Chl *a* analyses, to Else Torstensen (Institute of Marine Research) for cruise cooperation, and to two anonymous reviewers for valuable suggestion. This study was financially supported from the Norwegian Research Council (Project no. 196444/S40).

References

- Aarup, T., Holt, N., and Højerslev, N. K. 1996. Optical measurements in the North Sea-Baltic Sea transition zone. 2. Water mass classification along the Jutland west coast from salinity and spectral irradiance measurements. *Continental Shelf Research*, 16: 1343–1353.
- Aksnes, D. L., Dupont, N., Staby, A., Fiksen, Ø., Kaartvedt, S., and Aure, J. 2009. Coastal water darkening and implications for mesopelagic regime shifts in Norwegian fjords. *Marine Ecology Progress Series*, 387: 39–49.
- Aksnes, D. L., Ohman, M. D., and Riviere, P. 2007. Optical effect on the nitracline in a coastal upwelling area. *Limnology and Oceanography*, 52: 1179–1187.
- Alver, M. O., Hancke, K., Sakshaug, E., and Slagstad, D. 2014. A spectrally-resolved light propagation model for aquatic systems: steps toward parameterizing primary production. *Journal of Marine Systems*, 130: 134–146.
- Behrenfeld, M. J. 2010. Abandoning Sverdrup’s critical depth hypothesis on phytoplankton blooms. *Ecology*, 91: 977–989.
- Bissett, W. P., Carder, K. L., Walsh, J. J., and Dieterle, D. A. 1999. Carbon cycling in the upper waters of the Sargasso Sea: II. Numerical simulation of apparent and inherent optical properties. *Deep Sea Research I: Oceanographic Research Papers*, 46: 271–317.
- Branco, A. B., and Kremer, J. N. 2005. The relative importance of chlorophyll and colored dissolved organic matter (CDOM) to the prediction of the diffuse attenuation coefficient in shallow estuaries. *Estuaries*, 28: 643–652.
- Bricaud, A., Morel, A., and Prieur, L. 1981. Absorption by dissolved organic matter of the sea (yellow substance) in the UV and visible domains. *Limnology and Oceanography*, 26: 43–53.
- Chiswell, S. M. 2011. Annual cycles and spring blooms in phytoplankton: don’t abandon Sverdrup completely. *Marine Ecology Progress Series*, 443: 39–50.
- Dupont, N., and Aksnes, D. L. 2013. Centennial changes in water clarity of the Baltic Sea and the North Sea. *Estuarine Coastal and Shelf Science*, 131: 282–289.
- Fasham, M. J. R., Ducklow, H. W., and McKelvie, S. M. 1990. A nitrogen-based model of plankton dynamics in the oceanic mixed layer. *Journal of Marine Research*, 48: 591–639.
- Fleming-Lehtinen, V., and Laamanen, M. 2012. Long-term changes in Secchi depth and the role of phytoplankton in explaining light attenuation in the Baltic Sea. *Estuarine Coastal and Shelf Science*, 102–103: 1–10.
- Frigstad, H., Andersen, T., Hessen, D. O., Jeansson, E., Skogen, M., Nautsvoll, L. J., Miles, M. W., *et al.* 2013. Long-term trends in carbon, nutrients and stoichiometry in Norwegian coastal waters: evidence of a regime shift. *Progress in Oceanography*, 111: 113–124.
- Fujii, M., Boss, E., and Chai, F. 2007. The value of adding optics to ecosystem models: a case study. *Biogeosciences*, 4: 817–835.

- Gran, H. H., and Braarud, T. 1935. A quantitative study of the phytoplankton in the Bay of Fundy and the Gulf of Maine (including observations on hydrography, chemistry and turbidity). *Journal of the Biological Board of Canada*, 1: 279–467.
- Haraldsson, M., Tønnesson, K., Tiselius, P., Thingstad, T. F., and Aksnes, D. L. 2012. Relationship between fish and jellyfish as a function of eutrophication and water clarity. *Marine Ecology Progress Series*, 471: 73–85.
- Hjøllo, S. S., Huse, G., Skogen, M. D., and Melle, W. 2012. Modelling secondary production in the Norwegian Sea with a fully coupled physical/primary production/individual-based *Calanus finmarchicus* model system. *Marine Biology Research*, 8: 508–526.
- Holm-Hansen, O., Lorenzen, C., Holmes, R., and Strickland, J. 1965. Fluorometric determination of chlorophyll. *ICES Journal of Marine Science*, 30: 3–15.
- Højerslev, N. K., Holt, N., and Aarup, T. 1996. Optical measurements in the North Sea–Baltic Sea transition zone. 1. On the origin of the deep water in the Kattegat. *Continental Shelf Research*, 16: 1329–1342.
- Kirk, J. T. O. 2011. *Light and Photosynthesis in Aquatic Ecosystems*. Cambridge University Press, Cambridge.
- Kowalczyk, P., Cooper, W., Whitehead, R., Durako, M., and Sheldon, W. 2003. Characterization of CDOM in an organic-rich river and surrounding coastal ocean in the South Atlantic Bight. *Aquatic Sciences*, 65: 384–401.
- Kowalczyk, P., Olszewski, J., Darecki, M., and Kaczmarek, S. 2005. Empirical relationships between coloured dissolved organic matter (CDOM) absorption and apparent optical properties in Baltic Sea waters. *International Journal of Remote Sensing*, 26: 345–370.
- Larsen, S., Andersen, T., and Hessen, D. O. 2011. Climate change predicted to cause severe increase of organic carbon in lakes. *Global Change Biology*, 17: 1186–1192.
- Mei, Z. P., Saucier, F. J., Le Fouest, V., Zakardjian, B., Sennville, S., Xie, H. X., and Starr, M. 2010. Modeling the timing of spring phytoplankton bloom and biological production of the Gulf of St. Lawrence (Canada): effects of colored dissolved organic matter and temperature. *Continental Shelf Research*, 30: 2027–2042.
- Morel, A., and Maritorena, S. 2001. Bio-optical properties of oceanic waters: a reappraisal. *Journal of Geophysical Research: Oceans*, 106: 7163–7180.
- Mouw, C. B., Yoder, J. A., and Doney, S. C. 2012. Impact of phytoplankton community size on a linked global ocean optical and ecosystem model. *Journal of Marine Systems*, 89: 61–75.
- Nelson, N. B., and Siegel, D. A. 2013. The global distribution and dynamics of chromophoric dissolved organic matter. *Annual Review of Marine Science*, 5: 447–476.
- Roulet, N., and Moore, T. R. 2006. Environmental chemistry - browning the waters. *Nature*, 444: 283–284.
- Samuelson, A., Hansen, C., and Wehde, H. 2014. Tuning and assessment of the HYCOM NORWECOM V2.1 modeling System. *Geoscientific Model Development Discussion*, 7: 8399–8432.
- Sætre, R. 2007. *The Norwegian Coastal Current - Oceanography and Climate*. Tapir Academic Press, Trondheim.
- Sarmiento, J. L., and Gruber, N. 2006. *Ocean Biogeochemical Dynamics*. Princeton University Press, Princeton.
- Schrump, C., Alekseeva, I., and St John, M. 2006. Development of a coupled physical-biological ecosystem model ECOSMO - Part I: model description and validation for the North Sea. *Journal of Marine Systems*, 61: 79–99.
- Stedmon, C. A., and Markager, S. 2003. Behaviour of the optical properties of coloured dissolved organic matter under conservative mixing. *Estuarine Coastal and Shelf Science*, 57: 973–979.
- Stedmon, C. A., Markager, S., and Kaas, H. 2000. Optical properties and signatures of chromophoric dissolved organic matter (CDOM) in Danish coastal waters. *Estuarine Coastal and Shelf Science*, 51: 267–278.
- Sverdrup, H. U. 1953. On conditions for the vernal blooming of phytoplankton. *Journal du Conseil Permanent International pour l'Exploration de la Mer*, 18: 287–295.
- Urtizberea, A., Dupont, N., Rosland, R., and Aksnes, D. L. 2013. Sensitivity of euphotic zone properties to CDOM variations in marine ecosystem models. *Ecological Modelling*, 256: 16–22.
- Walsh, J. J., Weisberg, R. H., Dieterle, D. A., He, R. Y., Darrow, B. P., Jolliff, J. K., Lester, K. M., *et al.* 2003. Phytoplankton response to intrusions of slope water on the West Florida Shelf: Models and observations. *Journal of Geophysical Research-Oceans*, 108: 1–23.
- Yamashita, Y., and Tanoue, E. 2008. Production of bio-refractory fluorescent dissolved organic matter in the ocean interior. *Nature Geoscience*, 1: 579–582.

Handling editor: Shubha Sathyendranath